This article is published as: Vanmaercke M, Zenebe A, Poesen J, Nyssen J, Verstraeten G, Deckers J (2010) Sediment dynamics and the role of flash floods in sediment export from medium-sized catchments: a case study from the semi-arid tropical highlands in northern Ethiopia. Journals of Soils and Sediments 10: 611-627.

Sediment dynamics and the role of flash floods in sediment export from medium-sized catchments: a case study from the semi-arid tropical highlands in northern Ethiopia

Matthias Vanmaercke • Amanuel Zenebe • Jean Poesen • Jan Nyssen • Gert Verstraeten • Jozef Deckers

M. Vanmaercke (✉) • A. Zenebe • J. Poesen • G. Verstraeten • J. Deckers

Department of Earth and Environmental Sciences, K.U. Leuven, Celestijnenlaan 200 E, 3001 Heverlee, Belgium

e-mail: matthias.vanmaercke@ees.kuleuven.be

A. Zenebe

Department of Land Resources Management and Environmental Protection, Mekelle University, Mekelle, Ethiopia

J. Nyssen

Department of Geography, Ghent University, 9000 Gent, Belgium

Corresponding author:

Matthias Vanmaercke

Tel: +32 16 326420

Fax: +32 16 322980

matthias.vanmaercke@ees.kuleuven.be

Abstract

Purpose The Ethiopian highlands are a fragile environment, characterized by steep slopes, intense rainfall, a sparse vegetation cover and the occurrence of flash floods. Although important efforts have been made to mitigate the ongoing soil erosion and land degradation problems, the sediment dynamics at medium-sized catchment scale (100–10,000 km²)

are not fully understood. Therefore, this study aims to provide a better of sediment export processes and the importance of flash flood events in semi-arid tropical catchments.

Methods Measuring campaigns were conducted in 10 subcatchments of the Geba, a tributary of the Tekeze, representative of the northern Ethiopian highlands. During 2 to 4 rainy seasons, the rivers were sampled for their suspended sediment concentration (SSC) and runoff discharge.

Results and discussion Variations in SSC and sediment grain-size distribution indicate changes in sediment supply during the rainy season, due to the depletion of readily available sediments and the development of a vegetation cover. Also during flood events, changes in sediment supply are observed. Sediment yields (i.e. 497–6,543 t km^{-2} yr^{-1}) are higher than suggested by previous studies and correlate with rainfall depth. The majority of sediment export occurs during a few short but intense flash floods. No clear effect of implemented soil and water conservation measures could be detected in the sediment yields of the catchments.

Conclusions Sediment export rates in the Ethiopian highlands are high, are characterized by important changes in sediment supply and are mainly controlled by the occurrence and magnitude of flash flood events. Mitigation measures to reduce sediment yield at the catchment scale should therefore not only focus on the reduction of hillslope erosion rates, but also on the magnitude of these floods.

Keywords Catchment • Flash floods • Hysteresis • Suspended sediments • Sediment yield • Soil conservation

1 Introduction

Food production in Ethiopia is not able to support the increasing population due to the erratic rainfall and the fragile environment in combination with extreme poverty, stagnating technology, and high population and livestock densities (Ramakrishna and Demeke 2002; Nyssen et al. 2004a). Agriculture remains mainly rain-fed (Belete 2007) and, although the country is referred to as the 'water tower' of northeast Africa, it has one of the lowest reservoir storage capacities in the world (WCD 2000) and one of the lowest levels of electricity consumption per capita in the world, exploiting only 1–3% of its estimated 30,000 MW hydropower potential (Solomon 1998; Feibel 2003). Catching and storing runoff water in reservoirs is crucial to ensure food security and to provide hydropower energy. However, well-considered implementation of reservoirs is often impossible due to a lack of reliable sediment yield data, leading to reservoir sedimentation problems (Haregeweyn et al. 2008). Nyssen et al. (2004a) indicated that very few sediment yield data exist for medium-sized catchments (100-10,000 km^2) in the Ethiopian highlands.

The northern Ethiopian highlands represent a complex environment with a long history of human occupation, deforestation and severe problems of land degradation and soil erosion (Nyssen et al. 2004a). However, Ethiopia is also known for its numerous prevention, mitigation and land rehabilitation measures to reduce the on-site and off-site effects of soil erosion, such as the construction of stone bunds, check dams, exclosures and reforestation (Descheemaeker et al. 2006; Nyssen et al. 2007; Alemayehu et al. 2009). Although the potential of these rehabilitation measures to reduce runoff and soil erosion have been studied at the hillslope and small catchment scale (e.g. Descheemaeker et al. 2006; Haregeweyn et al. 2008; Nyssen et al. 2009a), the integrated effect of these measures at the medium-sized catchment scale is not well understood. The response of catchments to soil erosion and human interventions is often complex due to scale effects which can buffer changes in sediment supply (Walling 1983; Trimble 1999; Verstraeten et al. 2002; Walling 2006; de Vente et al. 2007). Further, many rivers in the northern Ethiopian highlands have a hydrological regime characterized by flash floods. Although flash floods often have a significant geomorphic impact, insight into the sediment export process during these events remains limited, due to their complex nature, difficulties to predict them and practical measuring problems (Baker et al. 1988).

Whereas sediment export measurements have been carried out worldwide (e.g. Jansson 1986; Syvitski and Milliman 2007), the majority of these studies were conducted in temperate or Mediterranean climates. For tropical environments, much less studies exist (e.g. Jansson 1986). In particular, the amount and quality of sediment export data from sub-Saharan Africa is generally very limited (Walling 1984, 1996).

Therefore, the overall objective of this study is to better understand sediment export processes in semi-arid tropical catchments and the importance of flash flood events for these sediment fluxes. Specific objectives are (i) to study changes in sediment supply of medium-sized catchments in the northern Ethiopian highlands at the seasonal scale as well as during single flash flood events; (ii) to assess the suspended sediment export of these catchments; and (iii) to identify the factors controlling this sediment export.

2 Study area

This study was conducted in the Geba catchment (**Fig. 1**), a tributary of the Tekeze. The Geba (5,133 km²) is part of the Blue Nile basin, and is representative for the bio-physical conditions in the northern Ethiopian highlands. Ten subcatchments of the Geba were studied. Catchment areas (A) varied between 121 and 4,592 km² (see Fig. 1 and **Table 1**). The catchments Suluh (SU), Genfel (GE), Agula (AG) and Ilala (IL) were monitored during 2004–2007. Upper Geba (UG), May Gabat (MY), Endaselassie (EN), Middle Geba (MG), Upper Tankwa (UT) and Lower Tankwa (LT)

were monitored during 2006–2007. Several of the studied catchments are nested. Suluh, Genfel, Agula and Ilala are tributaries of the Upper Geba. Upper Geba, May Gabat and Endaselassie are tributaries of Middle Geba. Furthermore, Upper Tankwa is a tributary of Lower Tankwa, which flows in to Geba a few hundred meters downstream of the Middle Geba gauging station (Table 1).

Altitude in the Geba catchment ranges from 3298 m a.s.l. to 938 m a.s.l. (Fig. 1 & Table 1). Geba's topography can be described as mountainous with plateaus deeply incised by the rivers. The climate in the Ethiopian highlands is complex with rainfall and air temperature varying with elevation (Nyssen et al. 2005). Annual rainfall in the Geba catchment varies around 600 mm but is characterized by large spatial and temporal variation. The majority of the annual rain falls in the summer rainy season (June–September) (**Fig. 2**), mainly during localized but intense convective storm events in the afternoon (Nyssen et al. 2005).

The intense convective rainfall, combined with the steep topography and often poor soil cover leads to a hydrologic regime that is characterized by flash floods. While runoff discharge is very small during most of the time, the majority of the water in the tributaries of the Geba is exported during flash floods. These floods mostly occur in the evening or night and often have a steep rising limb with flow depths rising from several centimeters to 3-8 meters in less than one hour (Zenebe 2009).

The geology of the Geba catchment consists of a basement complex plateau (metamorphic rocks) having an upper sedimentary rock layer (sandstone, shale, limestone, and limestone-marl) with some doleritic intrusions and capped by basalt trap series. Dominant lithologies of the studied subcatchments are shown in Table 1. The dominant soils in the Geba catchment are (lithic) Leptosols, mainly situated in the mountainous parts of the catchment. These shallow soils are not suitable for crop production, but are often cultivated due to a shortage of arable land. On more level lands, Cambisols, often with vertic properties, and Luvisols commonly occur. Fluvisols are found in some parts of the catchment, i.e. where alluvium is present along narrow incised river valleys (Zenebe 2009).

Land use is dominated by cultivated land, followed by bushed grass land and bare land (Table 1). Grasslands, forests, water bodies and built-up areas only cover small fractions of the catchments (Zenebe 2009). In many parts of the catchments soil and water conservation (SWC) measures have been applied to reduce runoff production and soil erosion. The most widely applied technique is the construction of stone bunds on hillslopes (Nyssen et al. 2007). Based on administrative data at the district level, an estimate of stone bund densities in each subcatchment was made (Table 1). These densities probably underestimate the true density of SWC structures, since no complete inventories of all applied SWC measures in the study area were available (Zenebe 2009).

3 Materials and methods

3.1 Field data collection

Runoff discharge and suspended sediment discharge were monitored at ten gauging stations in the Geba catchment (Fig. 1, Table 1). All fieldwork was carried out during the rainy seasons (July–September) of 2004–2007. A digital pressure transducer ('TD-diver') was installed at each station, recording the (water + atmospheric) pressure every 10 minutes. Barometric pressure transducers were installed at IL, MY and LT to allow correction for the atmospheric pressure of the TD-divers in these stations and their nearby stations. Each station was also equipped with a scaffold (allowing sampling during high water stages), a staff gauge and a shelter hut in corrugated steel.

In addition to the TD-diver recordings, manual measurements were made. In 2004, these were carried out 2-3 times per week. In 2005–2007 measurements were made at least daily and when a major change in flow depth was observed. To avoid bias on the estimation of the sediment export, data were collected as much as possible on a flow-proportional basis (Webb et al. 1995). Each measurement consisted of the manual reading of flow depth, determining instantaneous runoff discharge (Q, $m^3\ s^{-1}$) and sampling the suspended sediments. Q was determined using the area-velocity method (Bartram and Balance 1996; Zenebe 2009). Depth-integrated suspended sediment samples were taken to avoid bias (Bartram and Balance 1996). Due to strong currents, it was often impossible to sample the entire water column during floods. However, since the flow was very turbulent during these floods, a good mixing of the sediments can be expected, reducing errors to an acceptable level. After the volume was determined (generally around 400 ml), each sample was filtered (using Whatman filter papers with a pore opening of 2.5 µm). The remaining water after filtration was generally completely clear, indicating that the vast majority of the suspended solids were trapped by the filter paper. If the remaining water was still turbid, it was filtered again until it was clear. The filtered sediments were oven dried for 24 hours at 105°C and weighed. The suspended sediment concentration (SSC, $kg\ m^{-3}$) of each sample was determined as the mass of suspended sediment divided by the sample volume. In total 2,846 suspended sediment samples were analyzed (**Table 2**).

Sampling flash flood was dangerous and difficult since they mostly started after sunset at unpredictable moments. Because flow depths increased very rapidly during the rising limb of the floods, only five events could be sampled during both the rising and falling limb. Flash floods also destroyed several of the scaffolds, hampering further measurements, and washed out several TD-divers. This resulted in gaps in the continuous pressure series. Most problems occurred during the measurement campaign of 2006, when five out of ten scaffolds were destroyed and one

was severely damaged. In 2007, these problems were avoided by using a cable pulley system to take water samples and by installing the pressure transducers in iron boxes in the river bed instead of in the scaffolds.

3.2 Processing of the field data and calculation of the suspended sediment export

A double calibration procedure was followed to convert the continuous pressure series of the TD-divers to flow depths. The first calibration corrected for the air pressure and water temperature and was done automatically, using Van Essen Instruments Logger Data Manager ®. A comparison of the obtained flow depths with manually recorded flow depths revealed some important deviations. These deviations are mainly attributed to inaccuracies in manual measurements, since measuring flow depths during flash floods at night was often difficult. However, even when measurements taken during these circumstances are not considered, a systematic underestimation of 16% on the automatically recorded flow depths can still be observed. Therefore, a second calibration was performed to correct for this bias.

To convert the continuous flow depth series to runoff discharge series, depth-discharge relationships were developed between the manually measured instantaneous runoff discharges and their corresponding flow depth:

$$Q = r \times d^{s} \quad (1)$$

with d the calibrated flow depth (m) and r and s empirical constants. For all stations, good regression results were obtained with R^2 values varying between 0.91 and 0.99.

Sediment rating curves were developed in order to estimate SSC corresponding to the observed Q, as this is a widely applied method (e.g. Asselman, 2000; Morehead et al. 2003; Moliere et al. 2004):

$$SSC = a \times Q^{b} \quad (2)$$

where a and b are empirical constants. The empirical constants were determined using non-linear regression techniques to avoid biases due to logarithmic transformations of the data (Ferguson 1986; Asselman 2000).

Several studies show that the relationship between Q and SSC is often subject to a lot of scatter and variable at different temporal scales (e.g. Asselman 2000; Morehead et al. 2003; Moliere et al. 2004; Alexandrov et al. 2007). Also in this study, it was observed that the Q-SSC relationship is generally poor when all SSC-samples of a gauging station are considered. It was noted that for a given Q, SSC is generally much higher at the start of the rainy season than towards the end. Therefore, for each studied catchment, SSC-samples of all measuring campaigns were pooled and then stratified into three periods. Period 1 (P1) contains all samples taken before August 6th; period 2 (P2) contains all samples taken between August 6th and August 25th; period 3 (P3) consists of all samples taken after August 25th. This classification is rather arbitrary and it can be argued that a stratification based on a more physical basis, such as

cumulative rainfall, would be better. However, these dates were chosen as a trade off between describing the changing sediment dynamics as accurately as possibly and maintaining a sufficiently large number of SSC-samples to calculate reliable rating curves (**Table 3**). Other stratifications of SSC samples, e.g. based on cumulative rainfall depth, were tested but found to yield less reliable results.

Daily sediment export values were calculated as:

$$Q_{s,d} = \sum_{i=1}^{n} (Q_i \times SSC_i \times 600) \quad (3)$$

with $Q_{s,d}$ the daily sediment export (t day^{-1}); n the number of 10-minutes intervals per day (i.e. 144); Q_i the runoff discharge for each 10-minutes interval (m^3 s^{-1}), derived from the continuous flow depth series with Eq. 1; and SSC_i the corresponding, estimated SSC (kg m^{-3}) calculated with Eq. 2.

Total sediment export could then be calculated as the sum of all $Q_{s,d}$ values. At several stations TD-divers were washed away by flash floods, so $Q_{s,d}$ could not be calculated for some periods. When the number of days with missing diver records was limited (≤ 18 days), $Q_{s,d}$ was estimated using regression models. When the period was longer, no reliable sediment export could be calculated for that station and measuring campaign, as uncertainties were too large. The models first estimated the daily runoff discharge (Q_d, m^3 day^{-1}) for days without TD-diver data. For UG and MG this was done by making a regression between the observed Q_d at these stations and the sum of the observed Q_d values at the monitored upstream stations (with R^2 values of 0.73 and 0.80, respectively). For the stations AG, EN, UT and LT, missing Q_d values were predicted with a relationship between the calculated Q_d values and the daily maximum manually observed flow depth. These models had rather large uncertainties (R^2 values ranging between 0.33 and 0.64), but performed significantly better than models based on daily rainfall or the Q_d of nearby catchments. Missing $Q_{s,d}$ values were then predicted based on a regression between the observed Q_d and $Q_{s,d}$ values. Similar to the rating curves, only observed $Q_{s,d}$ values of the same period were considered for each station. R^2 values of these regressions ranged between 0.95 and 0.99.

3.3 Determination of the suspended sediment grain-size distribution

To better understand the sediment dynamics, the grain-size distributions of the suspended sediment samples were determined. Analysis of all suspended sediment samples was impossible, as the total number of samples was very large (n=2,846) and many of the samples did not contain enough sediment for grain-size analyses. Suspended sediment samples with an exceptionally high SSC (resulting in a sufficient mass of sediment, i.e. >10g) were analyzed separately.

The suspended sediment material of the other samples (with lower SSC values) was combined in different groups. This was done by stratifying all samples of one station and measuring campaign in three periods. The start and end dates of these periods were equal to those of the rating curves. Next, all samples within each period were sorted according to their SSC and plotted in a graph. Subgroups of 'low', 'medium' and 'high' SSC were then demarcated visually, based on observed natural breaks between the ranking and SSC of the samples. It was expected that this method would reveal trends in grain-size distribution as the differences in SSC were generally large and clear natural breaks were observed. In total 222 samples (169 grouped samples and 59 individual samples) were analyzed for their grain-size distribution, using the sieve-pipette method (Gee and Bauder 1986).

4 Results and discussion

4.1 Suspended sediment concentrations

Maximum SSC values are generally higher then those reported in other studies in semi-arid environments (e.g. Moliere et al. 2004; Seeger et al. 2004) (Table 2). However, Alexandrov et al. (2007) report concentrations in the same order of magnitude for flash floods in a 112 km² catchment in the Negev desert, Israel.

To evaluate the temporal variation in SSC, the Event Efficiency Index (EEI) of each SSC-sample was calculated. This index partly compensates for the fact that SSC increases with Q and can be interpreted as a measure of the efficiency of a runoff event to transport sediment. EEI (g s l^{-2}) was calculated as (Steegen et al. 2000):

$$EEI = \frac{SSC}{(Q/1000)} \quad (4)$$

The evolution of the EEI at Agula for all samples is displayed in **Fig. 3**. The other studied catchments have a similar pattern. In general, EEI is highly variable at the start of the rainy season with several peak values. When the rainy season proceeds, EEI values generally decrease and show less variability. Non-parametric Kruskal-Wallis tests confirm that the EEI values for P3 are significantly lower compared to P1 for all stations (p values <0.0001).

These changes are also reflected in the rating curves for the three periods (**Fig. 4** and Table 3). For a given Q, SSC is generally higher in P1 compared to P2 and P3. This is mainly attributed to the higher a-coefficients in the rating curves of P1 (Eq. 2), while the rating curves of P3 generally have higher b-exponents. Asselman (2000) suggested that the steepness of Q-SSC rating curves can be seen as a measure of the transport regime of a river. Flat rating curves (high a- and low b values) should be characteristic for river sections draining intensively weathered materials or loose sedimentary deposits, which can be transported at all discharges. Steep rating curves (low a- and high b values) should

be characteristic of rivers with little sediment transport taking place at low runoff discharges. An increase in runoff discharge results in a large increment of SSC, indicating that either the power of the river to erode material during high discharge periods is high, or that important sediment sources become available when the water level rises. Although Asselman (2000) indicates that differences in the steepness of rating curves can also be attributed to scale effects, this is not the case in this study since the rating curves only differ temporarily and not with catchment area. The observed changes in steepness are therefore most likely due to changes in sediment supply during the rainy season.

In the northern Ethiopian highlands, farmers are well aware of the high sediment loads in rivers at the beginning of the rainy season. Such water has a specific name, 'aigi' and is deemed to be nutritive, both for livestock and humans. There are several reasons to expect higher sediment availability at the start of the rainy season than towards its end. During the long dry season, a lot of soil material is detached by the large numbers of livestock, grazing on the plateaus and hillslopes. This loose material is washed out by the first runoff events to the river system. In addition, the cropland is generally sown at the beginning of the rainy season. At this time the fields have undergone at least two tillage operations, are bare and offer little resistance to splash and runoff erosion (Nyssen et al. 2009a). Due to the long dry season and the large numbers of grazing livestock, most hillslopes are almost bare at the start of the rainy season. However, after a few weeks of rain, a dense vegetation cover develops. A detailed study in the Agula catchment indicated that the vegetation cover increases from roughly 25% in the first half of July to over 65% in the second half of September (Hagos 2006). Several studies have already indicated that vegetation is crucial in reducing soil erosion rates and sediment delivery in the Ethiopian highlands, since it offers a better protection against splash and runoff erosion and traps part of the sediment before it enters the stream (e.g. Descheemaeker et al. 2006). A decrease in sediment supply due to the depletion of available material and/or the development of a better vegetative cover have been reported by various authors (e.g. Walling and Webb 1982; Hudson 2003; Moliere et al. 2004; Alexandrov et al. 2007). Furthermore, river baseflow generally increases towards the end of the rainy season (Zenebe 2009), but since baseflow does not contribute sediment to the river, the flow becomes diluted resulting in lower SSC values.

R^2 values of the rating curves are mostly very low, even when the data are stratified into three periods (Table 3). Many studies report hysteretic Q-SSC responses during flood events, explaining why a single Q-SSC relationship is subjected to large scatter (e.g. Williams, 1989; Hudson 2003; Moliere et al. 2004; Alexandrov et al. 2007). Hysteretic Q-SSC responses were also noted in this study (**Fig.5**). In the night of 26–27 August 2006, a large regional thunderstorm with rainfall depths of 30 to 40 mm caused large flash floods in most tributaries of the Geba catchment. According to farmers near the Upper Geba station, a flood of this magnitude was exceptional and did not occur during the preceding decade.

However, no historical data exist to confirm this. Multiple SSC-samples of the flood were taken at the Ilala station (see Fig. 5.1) and the Upper Geba station (see Fig. 5.2). For two samples at Upper Geba (indicated with a '?' in Fig. 5.2) Q and SSC were probably underestimated because water level exceeded the bankfull level at these times and measurements were carried out in the inundated floodplain, as close as possible to the river cross-section. Nevertheless, even without considering these two samples, our results indicate a positive (clockwise) hysteresis loop with SSC peaking before Q. A positive hysteresis was also observed at Ilala that night (Fig. 5.1). Clockwise hysteresis loops are commonly reported (e.g. Williams 1989; Hudson 2003; Moliere et al. 2004; Alexandrov et al. 2007) and are often related to the initial flushing of available sediment and (partial) exhaustion of sediment supplies. According to Williams (1989), this can occur either by: (a) a small sediment supply being available, or (b) a long-lasting and/or very intense flood. As the flood of 26–27 August 2006 occurred late in the rainy season and as it was of an exceptional magnitude, both conditions were met.

Although, the number of SSC-samples was limited, two consecutive flood events at the Ilala station in 2004 indicated a counterclockwise hysteresis response (Fig. 5.1). Counterclockwise hysteresis loops are generally less common (Williams 1989; Hudson 2003). Although different causes of counterclockwise loops, related to bank erosion, armour layers or rainfall characteristics, have been proposed by various authors (Williams 1989; Reid and Laronne 1995; Hudson 2003; Alexandrov et al. 2007), we have insufficient data to determine the exact cause of these loops. It is important to note, however, that the flood of 21–22 August 2004 shows only a limited hysteresis and could also be interpreted as an almost linear Q-SSC response. Linear responses for small events have been related to sediment depletion due to a previous event (Hudson 2003). This might also be the case for the flood of 21–22 August, as the flood occurred relatively late in the rainy season after a rather large flood event on 19–20 August (peak discharge of 88 $m^3 s^{-1}$).

During one flash flood at the LT-station (27–28 July 2007, Fig. 5.3) a figure-eight hysteresis loop was observed. According to Williams (1989) figure-eight loops can occur when an abundancy of sediment is available, so SSC peaks before Q but with post-peak sediment availability high enough so that SSC decreases relatively slower than Q. For the flood at LT the relatively high SSC values indeed suggest an abundancy of available sediment. Moreover, the flood occurred in P1, which is consistent with our finding that rating curves at the start of the rainy season indicate an abundancy of sediments. It should be noted, however, that SSC peaked after Q. This might be the result of different source areas contributing to Q and SSC at different times. As peak discharge was high, bank collapses might have

occurred during the flood, thereby delivering large amounts of sediment to river flow during the falling limb of the hydrograph.

4.2 Variation in suspended grain-size distributions

Table 4 gives an overview of the correlations between the average grain-size distribution of the analyzed grouped sediment samples and their corresponding catchment lithologies. Linear regressions were fitted between the average sand content (%, i.e. the fraction >50µm) of the analyzed sediment samples and the areal fraction of sandstone outcropping in the catchment (Table 1), and between the average clay content (%, i.e. the fraction <2 µm) and the areal fractions of 'clay-producing' lithologies. The areal fraction of clay-producing lithologies was defined as the sum of the fractions of limestone (LST), limestone-marls (LSM), shales (SHA) and basalts (BAS) outcropping in the catchment, since previous studies reported that these lithologies generally produce clayey soils in the study area (e.g. Abayneh et al. 2006; Van de Wauw et al. 2008).

When all grouped samples are considered, weak correlations are found between the sand and clay content of the sediment samples and the areal fraction of sandstone and clay-producing lithologies, respectively (Table 4). Subdivision of the grouped samples according to their SSC-class and period in the rainy season reveals some further trends. At the start of the rainy season (P1), there is no relation between the sediment clay content and the areal fraction of clay-producing lithologies or between the sand content and the fraction of sandstone. For P2 and P3 better correlations exist. In these periods, sediment clay content is generally lower for catchments with a low fraction of clay-producing lithologies, while sand content is generally higher in catchments with a large fraction of sandstone. This leads, on average, to higher sand contents towards the end of the rainy season. Samples with a high SSC (mostly taken during high runoff discharges) generally have a lower clay and a higher sand content than samples with a lower SSC. Also, the R^2 values of the regressions are generally much lower for high-SSC than for low-SSC samples.

These findings further indicate the depletion of sediments towards the end of the rainy season. The lack of correlation between texture and catchment lithology in P1 can be explained by the abundance of fine sediments on the hillslopes, available after the long dry season. Various authors reported that sediments from hillslopes, brought to the river system by runoff, often consists mainly of fine textures (e.g. Slattery and Burt 1997; Alexandrov et al. 2007; Seeger et al. 2004). As the rainy season proceeds, sediment becomes less readily available and grain-size distribution correlates better with catchment lithology. The depletion of fine sediments from the hillslopes, leads to on average higher sand contents towards the end of the rainy season. These sandy materials probably originate from sources close to or in the

river channel, as greater transport selectivity can be expected for coarser grains (e.g. Slattery and Burt 1997). Also Hudson (2003) reports a relatively greater importance of sandy bed material towards the end of the rainy season as a result of sediment depletion.

The generally higher sand content of samples with a high SSC agrees with the assumption that higher stream powers are needed to transport coarser fractions (Horowitz 1985), since SSC correlates positively with Q. However, some authors have reported no or an inverse relationship between mean sediment grain-size and runoff discharge, as suspended sediment is often mainly supply dependent and other sediment sources can become available during higher runoff discharges (e.g. Slattery and Burt 1997; Walling et al. 2000). This probably explains why the correlation coefficients are generally lower for high-SSC samples.

Some samples, taken during flash floods (Fig. 5), contained sufficient sediment and were analyzed separately for their grain-size distribution, allowing evaluation of the changes in grain-size distribution during single flood events. During the exceptional flood of 26-27 August 2006 at UG (Fig. 6 left), sand content decreased from almost 50% to less than 26% in less than 50 minutes, while silt and clay content increased. Also the samples taken at IL indicate an increase in the clay content during the rising limb of the flood, although sand content also slightly increases. This finding seems consistent with the process of sediment flushing, suggested by the clockwise hysteresis loop (Fig. 5.1 & 5.2). Walling et al. (2000) found evidence of a pulse of coarse sediment in the rising limb of storm events, which was related to the remobilization of coarse channel sediments as flow velocity and shear stress increased. The decrease in sand content at UG can therefore also possibly be related to the end of a pulse of coarse sediments or a combination of both mechanisms. Unfortunately, no other samples of the flood could be analyzed for their grain-size distribution. Also during the flood of 27–28 July 2007 at LT clear changes in suspended sediment texture were noted (Fig. 6, right). Texture became increasingly clayey during the rising limb of the flood, but was much sandier during the SSC-peak, occurring in the falling limb. This pattern is consistent with the hypothesis that the observed figure-eight loop is caused by a fast and high input of suspended sediments during the rising limb and a further increase in SSC during the falling limb due to the input of sediments from another source, such as bank collapses.

4.3 Sediment export rates and scale dependency

To allow comparison, all seasonal sediment export rates (**Table 5**) were calculated for the period from 12 July to 10 September. Data from measuring campaigns with insufficient TD-diver data were not included. To have an idea of the total annual sediment export, these sediment export rates were linearly extrapolated, considering the rainfall depth

during the measuring campaign and the annual rainfall depth in the catchment. These extrapolations induce extra uncertainty but are the best estimations of the yearly sediment yields that could be made, considering the available data. However, measurements were conducted for, on average, 62% of the annual rainfall depth and seasonal rainfall correlated reasonably well with the measured seasonal area-specific sediment yields (SSY-season, t km^{-2}), despite other controlling factors (**Fig. 7**). Therefore, the extra induced uncertainty is acceptable.

Calculated annual area-specific sediment yields (SSY, t km^{-2} yr^{-1}) range between 497 and 6,543 t km^{-2} yr^{-1}, and vary significantly between different years and subcatchments (see Table 5). **Fig. 8** shows the average SSY of all ten monitored subcatchments in relation to their catchment area (A, km^2). For comparison, other available SSY-data for catchments draining the Ethiopian highlands are included (Nyssen et al. 2004a; Haregeweyn et al. 2008). No significant relationship was found between A and SSY for the studied subcatchments of the Geba. Often, a negative relationship is expected due to a decrease in topsoil erosion rates on more gentle slopes and an increased probability for sediment deposition with increasing A. However, this relationship is frequently weak due to other controlling physical factors, so the fact that no relationship was found is not exceptional (Walling 1983; de Vente and Poesen 2005; de Vente et al. 2007). Nyssen et al. (2004a) found a significant negative relationship between A and SSY in Ethiopia. However, this relationship included almost no observations for medium-sized catchments (100–10,000 km^2). SSY values of this study are, on average, 3.8 times higher than this relationship would predict (Fig. 8). Moreover, it should be noted that the calculated SSY values of the Geba only consider suspended sediment load, whereas some of the data of Nyssen et al. (2004a) and all data of Haregeweyn et al. (2008) include bedload. After several flash floods channel aggradation at several gauging stations (i.e. SU, AG, UG, EN, UT and LT) was observed, indicating that bedload may be an important contributor to the total sediment load. A recent review by Turowski et al. (2010) indicates that the bedload fraction of sand bed rivers (such as SU) may be substantial (30-50% of the total sediment load). However, this conclusion was mainly based on data from temperate mountainous regions. Laronne and Reid (1993) reported that bedload transport in semi-arid ephemeral rivers is much more efficient than in their perennial counterparts of humid zones. Bedload may therefore contribute substantially to the total SSY of semi-arid tropical catchments. However, insufficient data exist to make an accurate estimation of bedload in the study area.

The higher than expected SSY for medium-sized catchments can probably be explained by the geomorphologic characteristics of the Ethiopian highlands. Comparable relationships between A and SSY have been reported for various regions (de Vente and Poesen 2005; de Vente et al. 2007). A trend line is added in Fig. 8 to illustrate this. The plateaus of the Ethiopian highlands are generally deeply incised by the larger river systems. Therefore, altitudinal differences

sharply increase as catchment area increases. Many of the small catchments (<100 km²) in Fig. 8 are situated on the plateaus and have a relatively limited difference in altitude. For example, the catchments of Haregeweyn et al. (2008), have an average height difference of 243 m (maximum: 561m, minimum: 80m) and an average slope gradient of 9.5%. The average height difference of the catchments in this study is 1,347 m (Table 1) and the average estimated slope gradient is 17.3%. Moreover, close to the river channels local slopes are often >100%. This steeper topography compensates for the fact that probability for sediment deposition increases with increasing sediment transport distance, leading to no significant decrease in SSY. As catchment areas further increase (>10,000 km²), the average terrain slope values decrease while the probability for sediment deposition further increases, leading to a decrease in SSY. Also floodplain sedimentation might contribute to this decrease as it was noted that the peak discharge of large flash floods often exceeds bankfull discharge. However, no quantitative data on floodplain sedimentation are available for the study area. In addition, the decrease in SSY is most probably enhanced by the fact that the area-specific runoff decreases with increasing catchment area, due to a decrease in average rainfall and runoff transmission losses (Zenebe 2009, Syvitski and Milliman 2007).

4.4 Factors controlling suspended sediment yield and the importance of flash floods

Although differences in SSY are often attributed to physical factors such as topography, lithology, land use and human interventions (e.g. Syvitski and Milliman 2007), Kendall Tau coefficients (τ) revealed no clear correlations between all SSY-season values (Table 5) and variables describing catchment topography, lithology or land use (Table 1). Only with the fraction of bushed grass land (BGL) was a significant (α=0.05) positive correlation found (τ = 0.37, p = 0.024). This relation is, however, not meaningful as it is very weak and mainly caused by the UT catchment, having high sediment yields and the largest fraction of BGL. There are several reasons for this lack of correlation. Firstly, uncertainties for the sediment export rates are large, due to the various measuring problems reported above. Also, the data used to describe the catchment characteristics are of low quality and have a low level of detail. Unfortunately better data were not available (Zenebe 2009).

But more important is probably the fact that spatially and temporally lumped parameters are inadequate to explain the distributed and time-varying nature of erosion and sediment transport (Walling 1983). While there is quite some similarity between the studied sub-catchments in terms of topography, land use and conservation efforts (Zenebe 2009; Table 1), rainfall patterns in the Ethiopian highlands are highly erratic (Nyssen et al. 2005). Seasonal rainfall showed a

significant and meaningful correlation with SSY-season (τ = 0.44, p = 0.005; Fig. 7), indicating that rainfall patterns are an important controlling factor of SSY. Cumulative distribution analyses of the continuous sediment export data indicate that roughly 50% of the sediment was exported during <5% of the measuring period. This clearly illustrates the high temporal variability in sediment export. Markus and Demissie (2006) found that the annual sediment export could be predicted, based on the sediment export of the largest flood events. Also in this study, a good correlation was found between the sediment yield of the largest flood event and SSY-season, demonstrating that the majority of sediments are exported by a limited number of flash flood events (**Fig. 9**). The occurrence and magnitude of these flash floods depend, however, mainly on local rainfall patterns and are difficult to predict (Zenebe 2009). The one to four year measuring periods of the studied catchments were too short to represent the variability of flash floods in each catchment. This might further explain why little of the variation in SSY-season between catchments could be explained by physical factors.

4.5 Suspended sediment yield, and soil and water conservation measures

Soil and water conservation (SWC) measures were found to have a profound impact on the SSY of small catchments in the Ethiopian highlands (Haregeweyn et al. 2008; Nyssen et al. 2009a). However, in this study, no significant correlation was found between all SSY-season values and the estimated stone bund (SB) density of each subcatchment (τ = -0.05, p = 0.784). However, as discussed earlier, uncertainties on the stone bund densities are large and a better correlation might be found when more detailed information on the SWC measures is available. Since SWC measures were applied in all the studied catchments, the contrast between the catchments might also be too small to generate a difference in SSY.

Although our results remain inconclusive about the effect of SWC-measures on the SSY of medium-sized catchments, the observed large temporal variations in sediment export suggest the need for an integrated approach of SWC-measures to reduce SSY. A large part of the yearly sediment export occurs during the first weeks of the rainy season due to the large sediment availability and the lack of a good vegetation cover. SWC-measures, such as stone bunds and exclosures, significantly reduce hillslope erosion and sediment connectivity (e.g. Descheemaeker et al. 2006; Nyssen et al. 2009a) and probably have a reducing effect on the sediment export at the beginning of the rainy season. A better, however still insignificant, correlation exists between the mass of sediments transported in P1 and SB density (τ = -0.26, p = 0.12). Sediment export is, however, mainly controlled by the occurrence of intense flash floods. On average 51% of the measured SSY was exported during P1, but this value varied between 10 and 90%, depending on the timing

of the largest floods. In order to reduce SSY, SWC-measures should therefore not only focus on the reduction of hillslope erosion rates, but also on the prevention of flood hazards by reducing peak flows.

The northern Ethiopian highlands have a long history of human occupation and deforestation (Nyssen et al. 2004a). Several river channels have widened since 1868 (Munro et al. 2008; Nyssen et al 2009b), which may be indicative of an increase in the occurrence and magnitude of flash floods, related to human interventions (Baker et al. 1988; Knighton 1998). However, since 1975 most river sections show no significant widening (Munro et al. 2008). This is probably partly the result of the many implemented SWC-measures, the recovery of vegetation and the improved soil protection that was noted over the past thirty years (Munro et al. 2008). Many of these measures, such as stone bunds and exclosures (Descheemaeker et al. 2008; Nyssen et al. 2010), check dams in gullies (Nyssen et al. 2004b) and the implementation of small reservoirs (Haregeweyn et al. 2008) also decrease storm runoff. The implemented SWC-measures therefore probably also have a significant effect on the reduction of sediment supply to river systems at the medium-sized catchment scale. However, several authors have reported that the response to changes in sediment supply at the catchment scale is often complex (Walling 1983, 2006; Trimble 1999; de Vente and Poesen 2005; de Vente et al. 2007). Other erosion and sediment deposition processes may override changes in sediment supply as scale increases from the hillslope to larger catchments. Munro et al. (2008) report that although soil erosion rates due to sheet and rill erosion rates have generally decreased, gullies show on average deeper channel incisions since 1975. The changes in Q-SSC response and sediment grain-size distribution, observed in this study, also suggest that other sediment sources become more important once the readily available sediments at the start of the rainy season are depleted. These complex responses may further explain why the effects of SWC measures are not clearly recognizable in the SSY. Evaluation of the effect of land use changes or SWC-measures on the SSY of medium-sized catchment should therefore consider all potential sediment sinks and sources, in particular gully and riverbank erosion as ephemeral channels are now in an incisional phase (Munro et al. 2008).

5 Conclusions

Measured sediment yields of medium-sized catchments in the northern Ethiopian highlands are higher than estimations of previous studies. Sediment export is characterized by a very large temporal variability. Changes in the relationship between runoff discharge and suspended sediments and changes in the suspended sediment grain-size distribution indicate important variations in sediment sources during the rainy season as well as during single flash flood events.

Sediment export rates are mainly controlled by the occurrence and magnitude of flash flood events and are difficult to predict, since these floods depend mainly on local rainfall patterns. Attempts to reduce sediment yield at the medium-sized catchment scale should therefore focus on the reduction of the magnitude of these floods.

Acknowledgments This study was conducted in the framework of VLIR-Mekelle University's IUC-Land Project (Belgium-Ethiopia). M. Vanmaercke received grant-aided support from the Research Foundation – Flanders (FWO), Belgium and K.U. Leuven. The help of Hailay Hagos, Kedir Mohammed, Kim Vanhulle, Annelies Beel, Isabelle Neyskens, Elke Soumillion and all other students and guards who helped with the collection and processing of the field data is gratefully acknowledged. Finally, this study benefited substantially from the comments by two anonymous reviewers and the editor.

References

Abayneh E, Zauyah Z, Hanafi M, Rosenani A (2006) Genesis and classification of sesquioxidic soils from volcanic rocks in sub-humid tropical highlands of Ethiopia. Geoderma 136:682–695

Alemayehu F, Taha N, Nyssen J, Girma A, Zenebe A, Behailu M, Deckers J, Poesen J (2009) The impacts of watershed management on land use and land cover dynamics in Eastern Tigray (Ethiopia). Resources, Conservation and Recycling 53:192–198

Alexandrov Y, Laronne J, Reid I (2007) Intra-event and inter-seasonal behaviour of suspended sediment in flash floods of the semi-arid northern Negev, Israel. Geomorphology 85:85–97

Asselman N (2000) Fitting and interpretation of sediment rating curves. J Hydrol 234:228–248

Baker V, Kochel R, Patton P (1988) Flood Geomorphology, Wiley-Interscience, New York

Bartram J, Balance R (1996) Water Quality monitoring – A practical Guide to the Design and implementation of Freshwater Quality Studies and Monitoring Programmes, E&FN Spon, London

Belete K (2007) Sedimentation and Sediment Handling at Dams in Tekeze River Basin, Ethiopia. Dissertation, Norwegian University of Science and Technology

Descheemaeker K, Nyssen J, Rossi J, Poesen J, Haile M, Raes D, Muys B, Moeyersons J, Deckers S (2006) Sediment deposition and pedogenesis in exclosures in the Tigray highlands, Ethiopia. Geoderma 132:291–314

Descheemaeker K, Poesen J, Borselli L, Nyssen J, Raes D, Haile M, Muys B, Deckers J (2008) Runoff curve numbers for steep hillslopes with natural vegetation in semi-arid tropical highlands, northern Ethiopia. Hydrol Process 22: 4097-4105

de Vente J, Poesen J (2005) Predicting soil erosion and sediment yield at the basin scale: Scale issues and semi-quantitative models. Earth-Sci Rev 71:95–125

de Vente J, Poesen J, Arabkhedri M, Verstraeten G (2007) The sediment delivery problem revisited. Prog Phys Geog 31:155–178

Feibel H (2003) An Interdisciplinary Approach to the Dissemination of Mini and Micro Hydropower—the case of Ethiopia. Dissertation, Darmstadt Terchnical University

Ferguson RI (1986) River Loads Underestimated by Rating Curves. Water Resour Res 22:74–76

Gee GW, Bauder JW (1986) Particle-size analysis. In: Klute A (ed) Methods of Soil Analysis: Part 1. Physical and Mineralogical Methods, 2nd edition., Soil Science Society of America, Madison, USA, pp 383–411

Hagos H (2006) Temporal variability of sediment discharge in relation to rainfall distribution and seasonal land cover variability throughout the rainy season in Agula catchment – Tigray, Ethiopia. MSc Dissertation, Mekelle University

Haregeweyn N, Poesen J, Nyssen J, Govers G, Verstraeten G, de Vente J, Deckers S, Moeyersons J, Haile M (2008) Sediment yield variability in northern Ethiopia: a quantitative analysis of its controlling factors. Catena 75:65–76

Horowitz AJ (1985) A Primer on Trace Metal-Sediment Chemistry. U.S. Geol Survey Water-Supply Paper 2277

Hudson PF (2003) Event sequence and sediment exhaustion in the lower Panuco Basin, Mexico. Catena 52:57–76

Jansson MB (1988) A Global Survey of Sediment Yield. Geogr Ann A 70:81–98

Knighton D (1998) Fluvial forms and processes: a new perspective. Arnold, London

Laronne JB, Reid I (1993) Very high rates of bedload sediment transport by ephemeral desert rivers. Nature 366:148-150

Markus M, Demissie M (2006) Predictability of annual sediment loads based on flood events. J Hydraul Eng-ASCE 11: 354–361

Moliere DR, Evans KG, Saynor MJ, Erskine WD (2004) Estimation of suspended sediment loads in a seasonal stream in the wet-dry tropics, northern Territory, Australia. Hydrol Process 18:531–544

Morehead MD, Syvitski J, Hutton EWH, Peckham SD (2003) Modeling the temporal variability in the flux of sediment from ungauged river basins. Global Planet Change 39:95–110

Munro RN, Deckers J, Haile M, Grove AT, Poesen J, Nyssen J (2008) Soil landscapes, land cover change and erosion features of the Central Plateau region of Tigrai, Ethiopia: Photo-monitoring with an interval of 30 years. Catena 75:55–64

Nyssen J, Poesen J, Moeyersons J, Deckers S, Haile M, Lang A (2004a) Human impact on the environment in the Ethiopian and Eritrean highlands—a state of the art. Earth-Sci Rev 64:273–320

Nyssen J, Veyret-Picot M, Poesen J, Moeyersons J, Haile M, Deckers J, Govers G, 2004b. The effectiveness of loose rock check dams for gully control in Tigray, Northern Ethiopia. Soil Use Manage 20: 55-64.

Nyssen J, Vandenreyken H, Poesen J, Moeyersons J, Deckers S, Haile M, Salles C, Govers G (2005) Rainfall erosivity and variability in the northern Ethiopian highlands. J Hydrol 311:172–187

Nyssen J, Poesen J, Gebremichael D, Vancampenhout K, D'aes M, Yihdega G, Govers G, Leirs H, Moeyersons J, Naudts J, Haregeweyn N, Haile M, Deckers S (2007) Interdisciplinary on-site evaluation of stone bunds to control soil erosion on cropland in northern Ethiopia. Soil Tillage Research 94:151–163

Nyssen J, Clymans W, Poesen J, Vandecasteele I, De Baets S, Haregeweyn N, Naudts J, Hadera A, Moeyersons J, Haile M, Deckers S (2009a) How soil conservation affects the catchment sediment budget - a comprehensive study in the north Ethiopian highlands. Earth Surf Proc Land 34:1216–1233

Nyssen J, Haile M, Naudts J, Munro N, Poesen J, Moeyersons J, Frankl A, Deckers S, Pankhurst R (2009b) Desertification? Northern Ethiopia re-photographed after 140 years. Sci Total Environ 407:2749–2755

Nyssen J, Clymans W, Descheemaeker K, Poesen J, Vandecasteele I, Vanmaercke M, Haile M, Nigussie Haregeweyn, Moeyersons J, Martens K, Zenebe A, Van Camp M, Tesfamichael Gebreyohannes, Deckers J, Walraevens K (2010) Impact of soil and water conservation on catchment hydrological response - a case in northern Ethiopia. Hydrol Process: in press.

Ramakrishna G, Demeke A (2002) An empirical analysis of food security in Ethiopia: The case of North Wello. Afr Dev 27:127–143

Reid I, Laronne J (1995) Bed load sediment transport in and ephemeral stream and a comparison with seasonal and perennial counterparts. Water Resour Res 31:773–781

Seeger M, Errea M, Beguería S, Arnáez J, Martí C, García-Ruiz JM (2004) Catchment soil moisture and rainfall characteristics as determinant factors for discharge/suspended sediment hysteretic loops in a small headwater catchment in the Spanish Pyrenees. J Hydrol 288:299–311

Slattery MC, Burt TP (1997) Particle size characteristics of suspended sediment in hillslope runoff and streamflow. Earth Surf Proc Land 22:705–719

Solomon S (1998) Hydropower in Ethiopia: Status, Potential and Prospects, Technical report, Ethiopian Association of Civil Engineers, Addis Ababa

Steegen A, Govers G, Nachtergaele J, Takken I, Beuselinck L, Poesen J (2000) Sediment export by water from an agricultural catchment in the Loam Belt of central Belgium. Geomorphology 33:25–36

Syvitski JPM, Milliman JD (2007) Geology, Geography, and Humans Battle for Dominance over the Delivery of Fluvial Sediment to the Coastal Ocean. J Geol 115:1–19

Trimble SW (1999) Decreased Rates of Alluvial Sediment Storage in the Coon Creek Basin, Wisconsin, 1975-93. Science 285:1244-1246

Turowski J, Rickenmann D, Dadson JS (2010) The partitioning of the total sediment load of a river into suspended load and bedload: A review of empirical data. Sedimentology: in press

Van de Wauw J, Baert G, Moeyersons J, Nyssen J, De Geyndt K, Taha N, Zenebe A, Poesen J, Deckers S (2008) Soil–landscape relationships in the basalt-dominated highlands of Tigray, Ethiopia. Catena 75:117–127

Verstraeten G, Van Oost K, Van Rompaey A, Poesen J, Govers G (2002) Evaluating an integrated approach to catchment management to reduce soil loss and sediment pollution through modeling. Soil Use Manage 19:386–394

Walling D (1983) The sediment delivery problem. J Hydrol 65:209–237

Walling DE (1984) The sediment yields of African rivers. In: Walling DE, Foster SSD, Wurzel P (eds) Challenges in African Hydrology and Water Resources (Proc Harare Symp), IAHS Publ. no. 144, IAHS Press, Wallingford, 265-283

Walling DE (1996) Hydrology and Rivers. In: Adams WE, Goudie AS, Orme AR (eds) The Physical Geography of Africa, Oxford University Press, pp 103–121

Walling DE (2006) Human impact on land–ocean sediment transfer by the world's rivers. Geomorphology 79:192–216

Walling DE, Webb BW (1982) Sediment availability and the prediction of storm-period sediment yields. In: Walling DE (ed) Recent Developments in the Explanation and Prediction of Erosion and Sediment Yield (Proc Exeter Symp), IAHS Publ. no. 137, IAHS Press, Wallingford, 327-337

Walling DE, Owens PN, Waterfall BD, Leeks GJL, Wass PD (2000) The particle size characteristics of fluvial suspended sediment in the Humber and Tweed catchments, UK. Sci Total Environ 252:205–222

WCD (2000) Dams and development. A new Framework for Decision Making. Report of the World Commission on Dams. Earthscan Publications, London

Webb B, Foster I, Gurnell A (1995) Hydrology, water quality and sediment behaviour. In: Foster I, Gurnell A, Webb BW (eds) Sediment and Water Quality in River Catchments, Wiley, Chichester, pp 1–18

Williams GP (1989) Sediment concentration versus water discharge during single hydrologic events in rivers. J Hydrol 111:89–106

Zenebe A (2009) Assessment of spatial and temporal variability of river discharge, sediment yield and sediment-fixed nutrient export in Geba River catchment, northern Ethiopia. Dissertation, Katholieke Universiteit Leuven

Figures

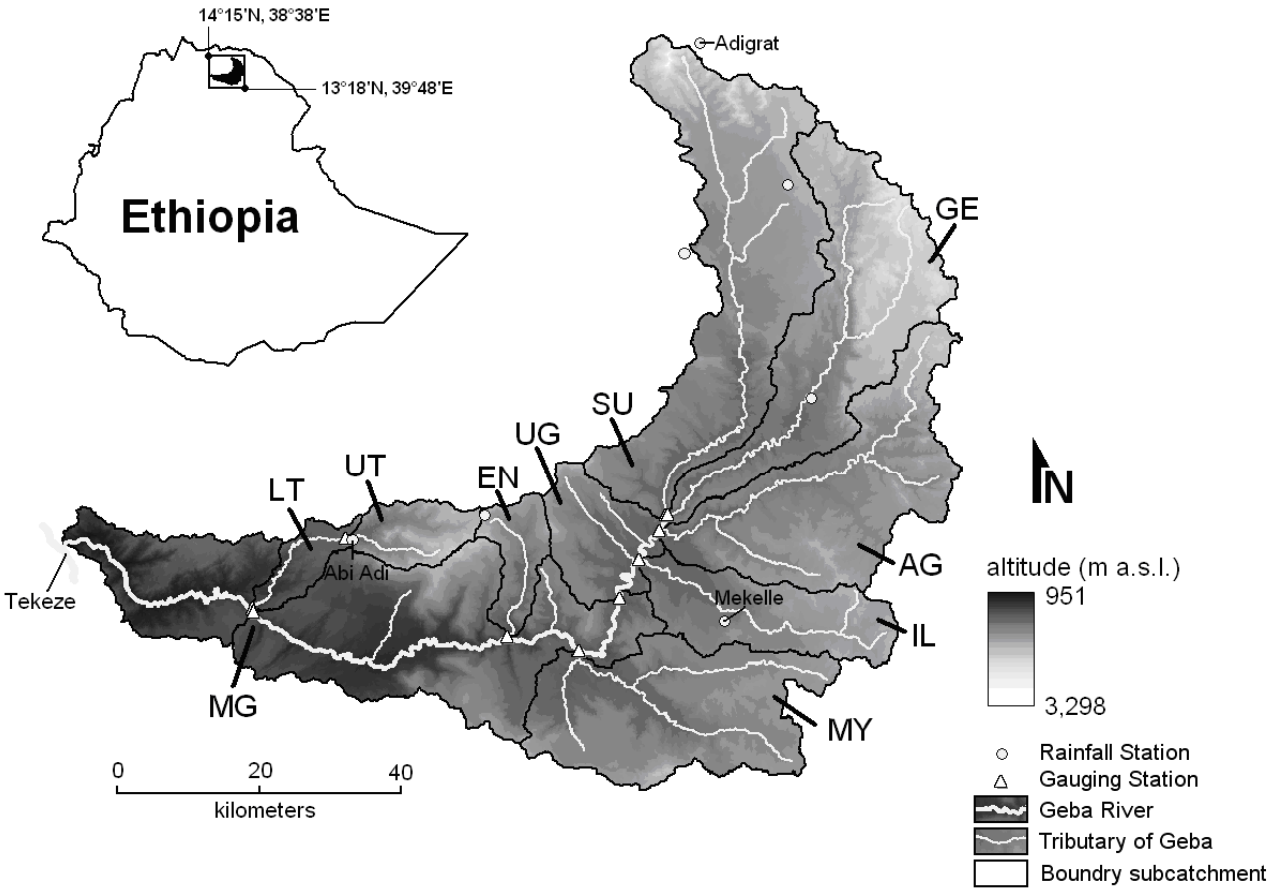

Fig. 1 Location and hydrology of the Geba catchment. See Table 1 for information on the catchment characteristics

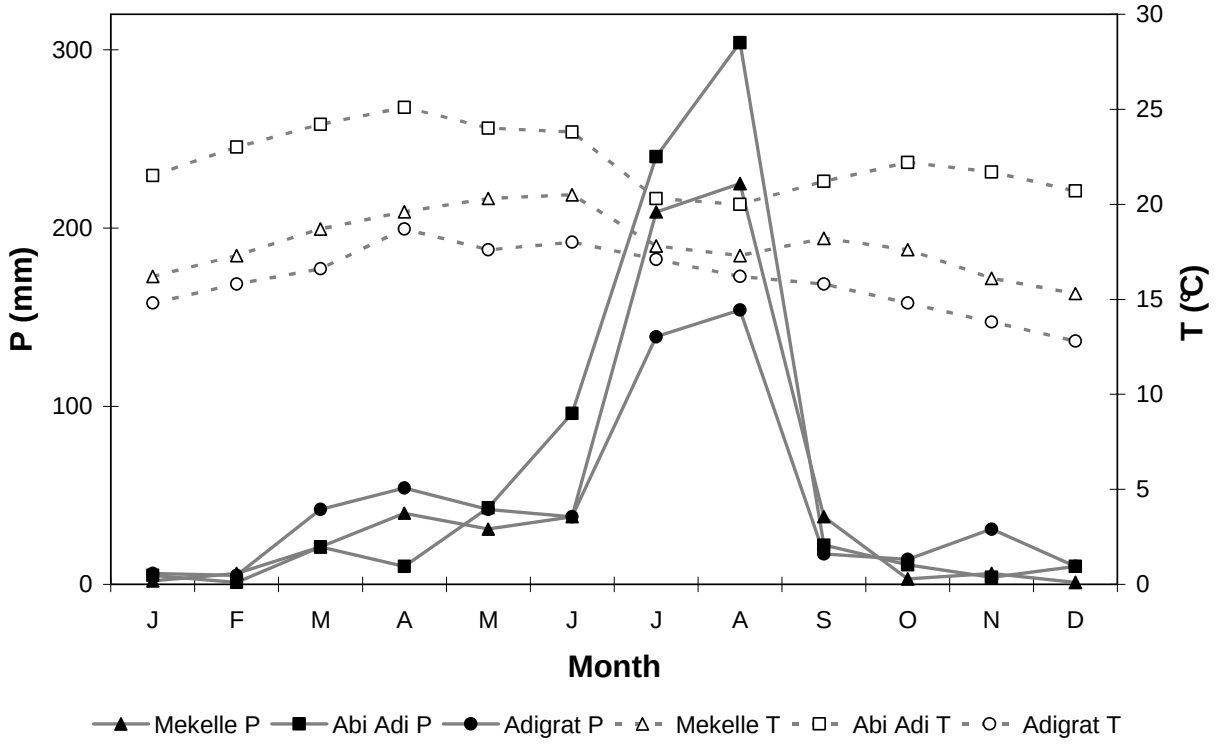

Fig. 2 Mean monthly rainfall (P, mm) and air temperature (T, °C) of Adigrat, Mekelle and Abi Adi weather stations (see Fig. 1). Data were obtained from the FAO NewLocClim database (1961-1991).

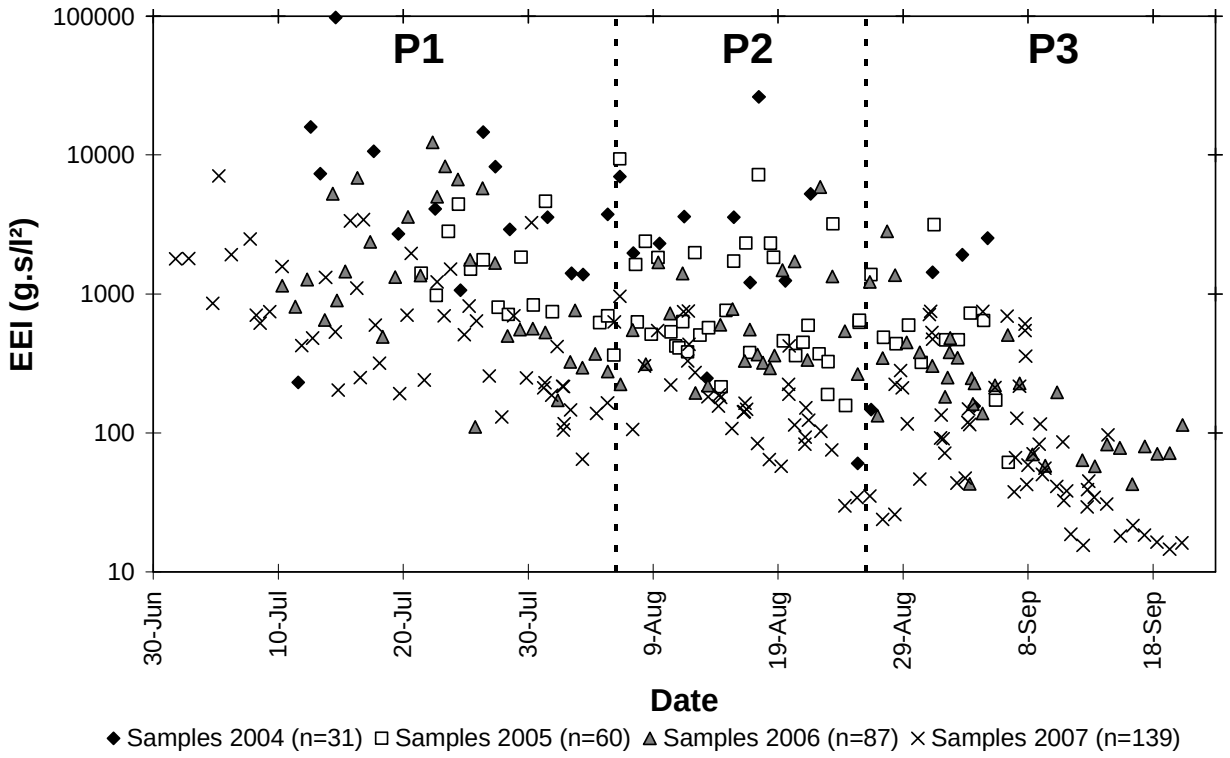

Fig. 3 Event Efficiency Indexes (EEI; eq. 4) of all SSC samples at Agula, taken during four rainy seasons

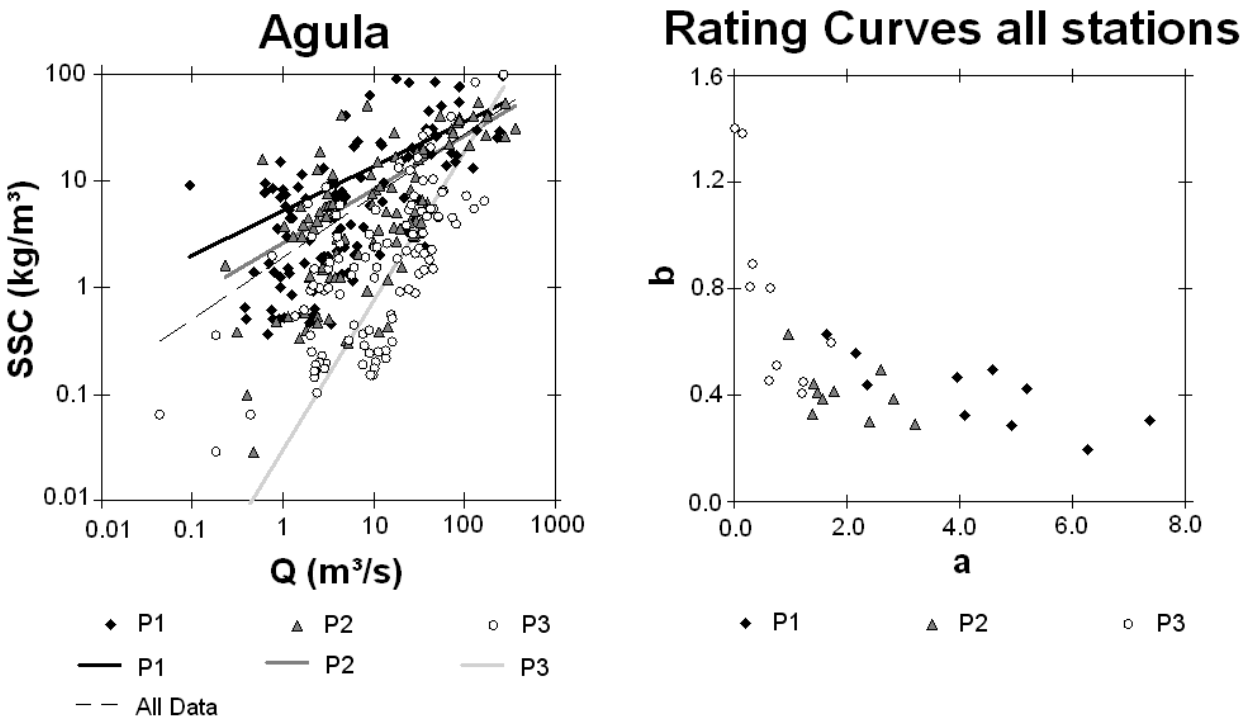

Fig. 4 Left: Example of the Q-SSC rating curves at the Agula station (Q=runoff discharge; SSC=Suspended Sediment Concentration). Right: coefficients a and b of the rating curves, subdivided per period (Table 3, Eq. 2). P1 groups all data collected before 6 August; P2 all data between 6-25 August; and P3 all data after 25 August

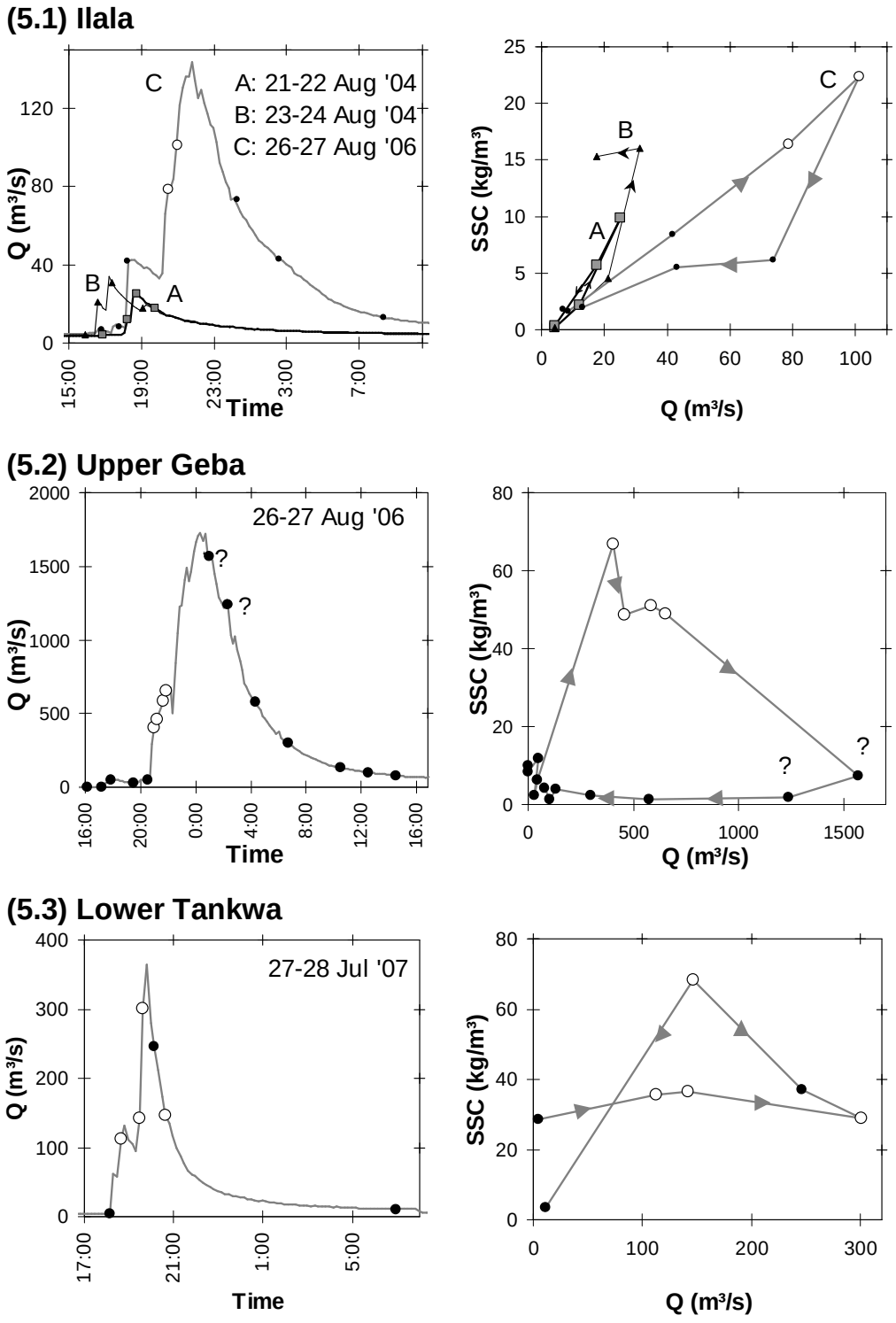

Fig. 5 Flood hydrographs (left) and Q-SSC response (right) of 5 sampled flash floods. Symbols indicate times and discharges when SSC-samples were taken. White circles indicate SSC-samples for which grain-size distribution was determined. The '?' indicate samples for which the Q and SSC is probably underestimated (see text)

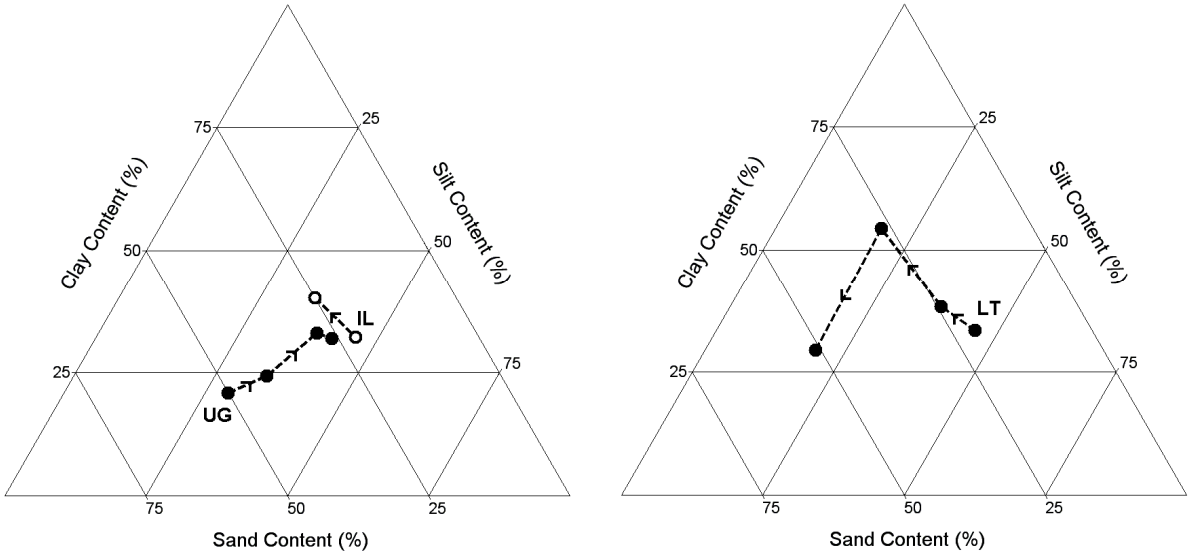

Fig. 6 Evolution of the suspended sediment texture during individual flood events. Left: grain-size data for the flash flood of 26-27 Aug 2006 at IL and UG. Right: grain-size data for the flash flood at LT on 27-28 July 2007. For details on the analyzed samples, see Fig. 5.

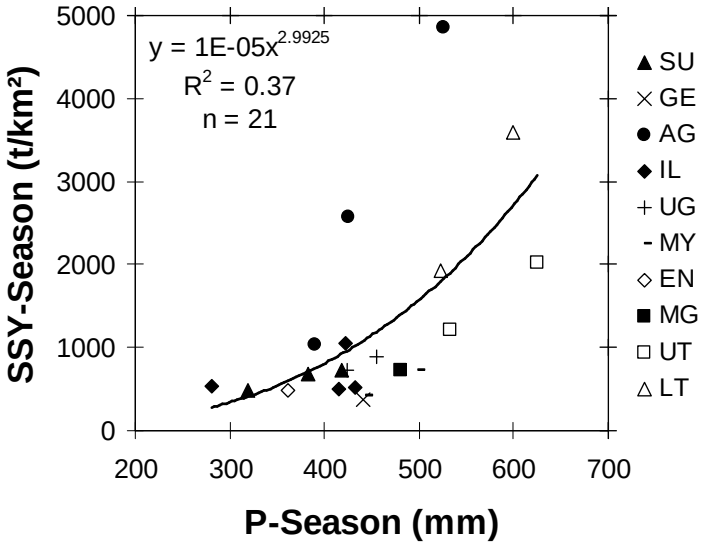

Fig. 7 Seasonal area-specific sediment yield (SSY-season) versus seasonal rainfall depth (P-Season) for all subcatchment and all measuring campaigns. For values, see Table 5

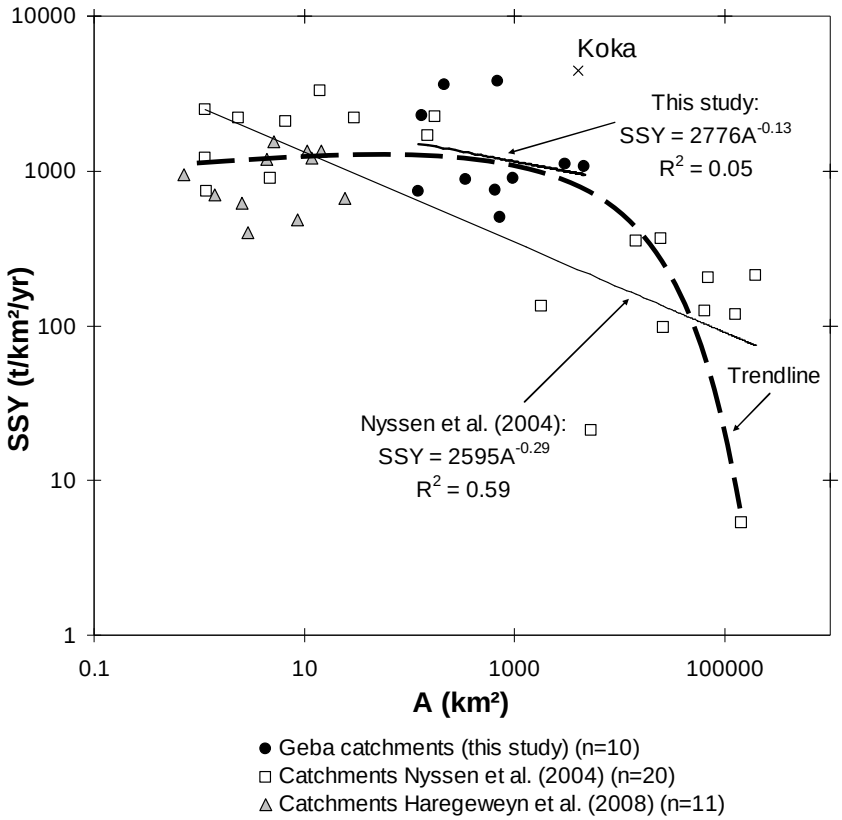

Fig. 8 Average sediment yield (SSY) in relation to their catchment area (A) (for values, see Table 5). Available sediment yield data from other studies were also included (Nyssen et al. 2004a; Haregeweyn et al. 2008). Data for Koka are probably overestimated and were not included in the regression analysis of Nyssen et al. (2004a). Trendline is obtained by free hand curve fitting.

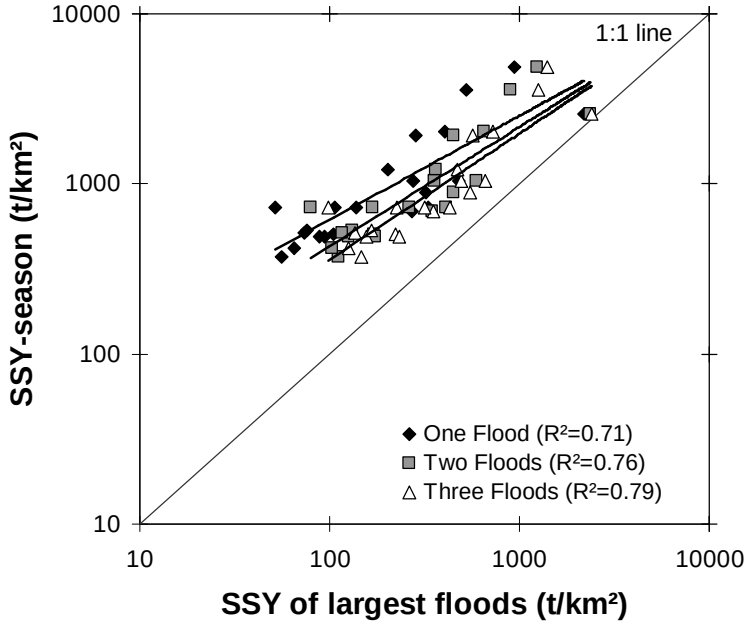

Fig. 9 Relations between the suspended sediment yield (SSY) of the largest one to three floods and the total seasonal sediment yield for all data of the 10 monitored subcatchments (n=21). For values, see Table 5.

Tables

Table 1 Main characteristics of the studied Geba subcatchments.

	Suluh	Genfel	Agula	Ilala	Upper Geba	May Gabat	Endaselassie	Middle Geba	Upper Tankwa	Lower Tankwa
Abbreviation	SU	GE	AG	IL	UG	MY	EN	MG	UT	LT
Station Location	13°38'57" N, 39°24'47" E	13°38'49" N, 39°25'07" E	13°37'31" N, 39°24'28" E	13°35'01" N, 39°23'19" E	13°32'27" N, 39°21'21" E	13°28'15" N, 39°17'51" E	13°29'30" N, 39°12'28" E	13°30'40" N, 38°53'41" E	13°36'55" N, 38°59'51" E	13°32'15" N, 38°53'34" E
Sampling years	2004-2007	2004-2007	2004-2007	2004-2007	2006-2007	2006-2007	2006-2007	2006-2007	2006-2007	2006-2007
A (km²)	969	733	692	341	3035	652	121	4592	130	216
Monitored tributaries	-	-	-	-	SU, GE, AG, IL	-	-	UG, MY, EN	-	UT
TOPOGRAPHY										
Hmin (m a.s.l.)	1777	1778	1764	1740	1702	1612	1484	1288	1814	1290
Hmax (m a.s.l.)	3298	3067	2859	2676	3298	2759	2812	3298	2824	2824
Hmean (m a.s.l.)	2320	2453	2280	2222	2312	2147	2157	2193	2362	2098
dH (m)	1521	1289	1095	936	1596	1147	1328	2010	1010	1534
Slope (%)	14.3	17.8	15.8	9.5	15.1	12.6	21	15.7	26.7	23.6
LITHOLOGY										
BAS (%)	7.6	0	0	0	2.5	0.1	5	2.4	42.3	25.6
DOL (%)	0	0	3	22.8	3.7	22	11.4	6.3	0	0
GRA (%)	4.8	0.2	0	0	1.6	0	0	1	0	0
LST (%)	23.1	13	47.1	19.3	29	27.9	55.5	30.8	0	0
LSM (%)	4.1	3.4	17.6	57.9	13.5	38.4	11.6	15.5	9.8	5.9
MET (%)	20.1	50.5	14.1	0	25.2	0	0	21.7	0.1	37.1
SST (%)	39.2	25.1	8.4	0	18.4	0.7	12.4	16.2	47.9	31.5
SHA (%)	1	7.8	9.8	0	6.1	10.8	4.1	5.9	0	0
LAND USE										
BaL (%)	26.3	20.9	20.1	13.2	21.5	11.1	23.9	18.6	9.3	10.1
BUA (%)	2.1	3.1	1.8	6.7	2.8	3.7	0.4	2.9	0.5	4.5
BGL (%)	22.3	27.1	24.9	13.5	24.1	18.4	33.3	24.9	48.7	37.1
CL (%)	39.7	39.4	40.7	60.8	41.9	62.8	27.1	45.2	30	40.1
FL (%)	0.3	0.4	1	0.3	0.5	0.3	0.7	0.4	1.8	1.3
GL (%)	9.3	9	11.5	5.1	9.1	3.5	14.6	7.8	9.6	6.8
WB (%)	0.1	0.1	0	0.4	0.1	0.1	0.1	0.1	0.1	0.2
SB density (km/km²)	4.0	3.8	4.2	5.6	4.1	4.0	3.2	3.8	3.3	3.1

A: catchment area; Hmin: minimum altitude in subcatchment; Hmax: maximum altitude in subcatchment; dH: Hmax-Hmin; Slope: average slope gradient; BAS: trap basalts; DOL: dolerite; GRA: granite; LST: limestone; LSM: limestone-marls; MET: metamorphic rocks; SST: sandstone; SHA: shales; BaL: bare land; BUA: built-up area; BGL: bushed grass land; CL: cultivated land; FL: forest land; GL: grass land; WB: water bodies; SB density: stone bund density.

Table 2 Characteristics of suspended sediment concentrations (SSC) and runoff discharges (Q). See Table 1 for station abbreviations.

Catchment	# samples	min SSC (kg/m³)	median SSC (kg/m³)	mean SSC (kg/m³)	max SSC (kg/m³)	min sampled Q (m³/s)	median sampled Q (m³/s)	mean sampled Q (m³/s)	max sampled Q (m³/s)
SU	318	0.06	2.93	5.02	43.02	0.02	9.84	18.96	345.89
GE	304	0.02	1.66	3.06	40.24	0.01	3.66	14.78	446.51
AG	317	0.03	3.78	9.96	96.69	0.04	10.51	26.51	370.40
IL	324	0.03	2.45	5.18	61.77	0.43	6.59	17.85	220.97
UG	319	0.12	4.78	6.89	49.28	0.00	10.76	25.04	471.53
MY	253	0.14	1.82	4.89	63.51	0.48	4.58	9.08	247.27
EN	267	0.00	1.57	5.93	106.44	0.03	0.77	9.23	221.08
MG	247	0.32	10.07	11.96	42.08	13.40	69.36	156.86	1489.38
UT	229	0.00	1.75	5.75	42.27	0.42	7.24	19.87	932.49
LT	268	0.00	3.95	9.39	68.36	0.49	8.11	25.64	332.83

Table 3 Overview of the Q-SSC rating curves. a and b are the coefficients of Eq. 2. "All samples" represents the regression result of all SSC-samples. P1, P2 and P3 represent the regression results for SSC-samples collected during three periods (P1, start of data to 5 August; P2, 6-25 August; P3, 26 August to end of data)

Catchment	group	# obs	a	b	R^2
SU	All samples	318	1.87	0.40	0.19
	P1	98	4.10	0.32	0.31
	P2	116	1.41	0.44	0.24
	P3	104	0.77	0.51	0.25
GE	All samples	304	1.42	0.40	0.32
	P1	82	2.36	0.44	0.52
	P2	119	1.47	0.41	0.37
	P3	103	0.62	0.45	0.48
AG	All data	317	1.88	0.58	0.35
	P1	110	5.18	0.42	0.36
	P2	101	2.61	0.50	0.52
	P3	106	0.03	1.40	0.57
IL	All samples	324	1.10	0.61	0.41
	P1	112	2.17	0.56	0.48
	P2	99	0.96	0.63	0.59
	P3	113	0.28	0.80	0.80
UG	All samples	229	2.85	0.32	0.16
	P1	79	4.93	0.29	0.24
	P2	72	2.40	0.30	0.27
	P3	78	1.25	0.45	0.19
MY	All samples	253	1.41	0.68	0.50
	P1	71	3.94	0.47	0.51
	P2	79	1.40	0.33	0.06
	P3	103	0.16	1.38	0.86
EN	All samples	267	2.69	0.57	0.57
	P1	103	4.58	0.49	0.62
	P2	64	2.83	0.39	0.44
	P3	100	1.72	0.60	0.68
MG	All samples	247	3.56	0.27	0.17
	P1	105	6.27	0.20	0.14
	P2	59	3.21	0.29	0.24
	P3	83	1.22	0.40	0.21
UT	All samples	229	1.95	0.48	0.47
	P1	67	1.63	0.63	0.79
	P2	58	1.78	0.41	0.45
	P3	104	0.66	0.80	0.33
LT	All samples	268	2.12	0.52	0.31
	P1	119	7.37	0.30	0.42
	P2	58	1.57	0.39	0.19
	P3	91	0.33	0.89	0.59

Table 4 Relationships of the average grain-size distribution of the suspended sediment samples and their corresponding catchment lithologies. ‘a’ and ‘b’ are the coefficients of the equation: y = ax+b. For clay, y is the average clay content (%) of the suspended sediment samples and x is the total areal fraction (%) of ‘clay producing’ lithologies (LST+LSM+BAS+SHA, see Table 1 and text). For sand, y is the average sand content (%) of the sediment samples and x is the areal fraction (%) of sandstone. Stratification of collected samples in three periods (P1, P2 and P3) and according to SSC groups (low, medium, high): see text

	Relation Clay content - 'Clay-producing' lithologies			Relation Sand content - Sandstone		
	a	b	R^2	a	b	R^2
All samples	0.12	38.1	0.26	0.16	11.0	0.25
P1	0.01	46.5	0.00	0.10	10.8	0.06
P2	0.26	31.6	0.45	0.26	7.7	0.53
P3	0.24	29.2	0.29	0.19	13.6	0.21
low SSC	0.24	39.2	0.47	0.21	4.5	0.61
medium SSC	0.14	38.8	0.22	0.18	7.9	0.46
high SSC	0.07	35.4	0.07	0.21	14.4	0.23
P1 - low SSC	0.01	55.1	0.00	0.01	5.6	0.01
P1 - medium SSC	0.01	49.4	0.00	0.16	5.7	0.38
P1 - high SSC	0.02	37.5	0.00	0.13	13.9	0.04
P2 - low SSC	0.34	33.7	0.57	0.26	3.6	0.47
P2 - medium SSC	0.24	31.7	0.41	0.30	5.1	0.87
P2 - high SSC	0.16	32.6	0.12	0.18	13.9	0.25
P3 - low SSC	0.36	28.7	0.69	0.35	4.6	0.57
P3 - medium SSC	0.17	34.2	0.07	0.08	13.6	0.02
P3 - high SSC	0.14	30.1	0.15	0.50	14.6	0.38

Table 5 Overview of the calculated sediment export rates. $Q_{s,\ season}$: total sediment export between 12 July and 10 September; $Q_{s,\ pred.}$: fraction of $Q_{s,\ season}$ that was predicted because of gaps in the TD-diver series (see text); P-season: total rainfall depth between 12 July and 10 September; P-year: total annual rainfall depth; P-measured: fraction of total rainfall that fell during the measuring campaign; SSY-season: measured area-specific sediment yield; SSY: extrapolated annual area-specific sediment yield.

Catchment	Year	Qs,season (t)	Qs, pred. (%)	P-season (mm)	P-year (mm)	P-measured (%)	SSY-season (t/km²)	SSY (t/km²/yr)
SU	2004	4.77E+05	0%	319	497	64%	492	669
	2005	-	-	-	-	-	-	-
	2006	7.02E+05	0%	418	690	61%	724	1010
	2007	6.63E+05	0%	383	694	55%	684	991
	Avg.	**6.14E+05**	**0%**	**373**	**627**	**60%**	**634**	**890**
GE	2004	-	-	-	-	-	-	-
	2005	-	-	-	-	-	-	-
	2006	2.74E+05	0%	441	656	67%	374	497
	2007	-	-	-	-	-	-	-
	Avg.	**2.74E+05**	**0%**	**441**	**656**	**67%**	**374**	**497**
AG	2004	-	-	-	-	-	-	-
	2005	7.16E+05	0%	390	531	73%	1035	1309
	2006	1.79E+06	3%	425	661	64%	2580	3500
	2007	3.36E+06	0%	525	804	65%	4860	6543
	Avg.	**1.95E+06**	**1%**	**447**	**665**	**67%**	**2825**	**3784**
IL	2004	1.81E+05	0%	280	390	72%	532	682
	2005	1.73E+05	0%	416	598	70%	508	663
	2006	1.76E+05	0%	432	691	62%	515	708
	2007	3.58E+05	0%	422	693	61%	1050	1460
	Avg.	**2.22E+05**	**0%**	**387**	**593**	**65%**	**651**	**878**
UG	2006	2.21E+06	2%	423	670	63%	729	997
	2007	2.71E+06	0%	455	716	64%	894	1220
	Avg.	**2.46E+06**	**1%**	**439**	**693**	**63%**	**811**	**1109**
MY	2006	2.73E+05	0%	443	683	65%	418	565
	2007	4.74E+05	0%	499	706	71%	727	940
	Avg.	**3.73E+05**	**0%**	**471**	**695**	**68%**	**572**	**752**
EN	2006	5.92E+04	25%	362	720	50%	489	733
	2007	-	-	-	-	-	-	-
	Avg.	**5.92E+04**	**25%**	**362**	**720**	**50%**	**489**	**733**
MG	2006	-	-	-	-	-	-	-
	2007	3.36E+06	7%	481	884	54%	732	1065
	Avg.	**3.36E+06**	**7%**	**481**	**884**	**54%**	**732**	**1065**
UT	2006	1.57E+05	41%	534	947	56%	1206	1732
	2007	2.63E+05	0%	626	1025	61%	2023	2812
	Avg.	**2.10E+05**	**20%**	**580**	**986**	**59%**	**1614**	**2272**
LT	2006	4.17E+05	17%	522	820	64%	1931	2633
	2007	7.75E+05	0%	600	842	71%	3587	4620
	Avg.	**5.96E+05**	**8%**	**561**	**831**	**67%**	**2759**	**3627**